

Enhancement of the Jahn-Teller distortion by magnetization in manganites

Y. Y. Chu, H. H. Wu, S. C. Liu, Hsiu-Hau Lin, J. Matsuno et al.

Citation: *Appl. Phys. Lett.* **100**, 112406 (2012); doi: 10.1063/1.3691946

View online: <http://dx.doi.org/10.1063/1.3691946>

View Table of Contents: <http://apl.aip.org/resource/1/APPLAB/v100/i11>

Published by the [American Institute of Physics](#).

Related Articles

Reliable nucleation of isolated magnetic antivortices

Appl. Phys. Lett. **100**, 162404 (2012)

Mn₂PtIn: A tetragonal Heusler compound with exchange bias behavior

Appl. Phys. Lett. **100**, 152404 (2012)

Origin of ferromagnetism and oxygen-vacancy ordering induced cross-controlled magnetoelectric effects at room temperature

J. Appl. Phys. **111**, 073904 (2012)

Spherical sample holders to improve the susceptibility measurement of superparamagnetic materials

Rev. Sci. Instrum. **83**, 045106 (2012)

Piezoresponse force microscopy and vibrating sample magnetometer study of single phased Mn induced multiferroic BiFeO₃ thin film

J. Appl. Phys. **111**, 064110 (2012)

Additional information on *Appl. Phys. Lett.*

Journal Homepage: <http://apl.aip.org/>

Journal Information: http://apl.aip.org/about/about_the_journal

Top downloads: http://apl.aip.org/features/most_downloaded

Information for Authors: <http://apl.aip.org/authors>

ADVERTISEMENT

<p>INSTRUMENTS FOR ADVANCED SCIENCE</p> 	<p>Gas Analysis</p> <p>dynamic measurement of reaction gas streams catalysis and thermal analysis molecular beam studies dissolved species probes fermentation, environmental and ecological studies</p>	<p>Surface Science</p> <p>UHV TPD SIMS end point detection in ion beam etch elemental imaging - surface mapping</p>	<p>Plasma Diagnostics</p> <p>plasma source characterisation etch and deposition process reaction kinetic studies analysis of neutral and radical species</p>	<p>Vacuum Analysis</p> <p>partial pressure measurement and control of process gases reactive sputter process control vacuum diagnostics vacuum coating process monitoring</p>
	<p>contact Hiden Analytical for further details: info@hiden.co.uk www.HidenAnalytical.com</p> <p>CLICK TO VIEW OUR PRODUCT CATALOGUE</p>			

Enhancement of the Jahn-Teller distortion by magnetization in manganites

Y. Y. Chu,^{1,2} H. H. Wu,² S. C. Liu,² Hsiu-Hau Lin,³ J. Matsuno,⁴ H. Takagi,^{4,5} J. H. Huang,¹ J. van den Brink,⁶ C. T. Chen,² and D. J. Huang^{2,3,a)}

¹Department of Materials Science and Engineering, National Tsing Hua University, Hsinchu 30013, Taiwan

²National Synchrotron Radiation Research Center, Hsinchu 30076, Taiwan

³Department of Physics, National Tsing Hua University, Hsinchu 30013, Taiwan

⁴Advanced Science Institute, RIKEN, Wako, Saitama 351-0198, Japan

⁵Department of Advanced Materials, University of Tokyo, Kashiwa, Chiba 277-8561, Japan

⁶Institute for Theoretical Solid State Physics, IFW Dresden, D-01171 Dresden, Germany

(Received 23 November 2011; accepted 13 February 2012; published online 15 March 2012)

Using measurements of resonant x-ray scattering from a $\text{LaMnO}_3/\text{SrMnO}_3$ superlattice grown on $\text{SrTiO}_3(001)$, we present experimental evidence for the enhancement of the Jahn-Teller distortion by magnetic ordering in manganites. With a specially tuned periodicity of the superlattice, scattering due to the Jahn-Teller (JT) distortion is separated from charge and magnetic scattering. The measured JT distortion is markedly enhanced upon the emergence of magnetization and strongly correlated with the spin ordering in the superlattice. Such strong correlation reveals the nature of electron-electron interaction for orbital ordering in manganites. © 2012 American Institute of Physics. [<http://dx.doi.org/10.1063/1.3691946>]

Understanding of the interplay between spin, charge, and orbital degrees of freedom is important to engineer the emergent physical properties transition-metal compounds.¹ Perovskite LaMnO_3 is a prototypical example showing cooperative Jahn-Teller (JT) distortions and orbital ordering. Two mechanisms have been proposed to explain the orbital ordering in manganites: electron-phonon coupling² and superexchange interaction.³ The electron-phonon coupling can cause the JT distortions first,⁴⁻⁶ and the orbital polarization is further enhanced by Coulomb repulsion.⁷ In the second scenario, the many-body superexchange interaction, originating from the degenerate e_g orbitals, drives the orbital ordering and in turn leads to JT distortions.⁸⁻¹⁰ To reveal the origin of orbital ordering in manganites, it is decisive to investigate the correlation between JT distortion and spin ordering, which is only remotely related to the electron-phonon interactions. Such correlation in most systems is obscured by other and more profound magnetic effects, so is difficult to observe.

L-edge resonant x-ray scattering of transition-metal compounds provides an effective means to resolve this conundrum.¹¹⁻¹³ With a synthetic superlattice, one can separate the contribution of orbital ordering in resonant x-ray scattering from that of charge scattering. Because the cross section of charge scattering of x-rays scales with $(\epsilon_1 \cdot \epsilon_2)^2$ in which the polarizations of incident and scattered x-rays are ϵ_1 and ϵ_2 , respectively, the cross section of charge scattering can be strongly suppressed by suitably tuning the angle between ϵ_1 and ϵ_2 . Such control is possible in artificial superlattices. The relative contribution of orbital scattering thus becomes separated.

In this letter, based on the measurements of resonant soft-x-ray scattering, we report the temperature dependence of the magnetic structures and the JT distortion in a $(\text{LaMnO}_3)_n/(\text{SrMnO}_3)_n$ superlattice with n being the periodicity. To suppress the contribution of charge scattering, we

tuned the superlattice such that the scattering angle 2θ is close to 90° , e.g., $n = 4$. The JT distortion is correlated with the magnetic order and follows a similar dependence on temperature. Although the local JT distortion is likely due to the electron-phonon interaction, our measurements provide evidence for many-body origin of the orbital ordering in manganites.

The $(\text{LaMnO}_3)_4/(\text{SrMnO}_3)_4$ superlattice was epitaxially grown by pulsed laser deposition on a $\text{SrTiO}_3(001)$ substrate cut with a surface normal tilted by 0.3° toward the a axis, and the repetition for the superstructure was 30. The soft-x-ray scattering measurements were performed by using the beamline 05B3 of the National Synchrotron Radiation Research Center, Taiwan. The scattering plane in which momentum transfer \mathbf{q} lies is defined by the a and c axes, i.e., $\mathbf{q} = (q_a \ 0 \ q_c)$ in units of $(\frac{2\pi}{a} \ \frac{2\pi}{a} \ \frac{2\pi}{\Lambda})$, in which $a = 3.905 \text{ \AA}$ is the lattice parameter of the substrate and Λ is the periodicity of the superlattice, i.e., $\Lambda \approx 8a$. The electric vector of incident soft x-rays is switchable to be parallel (perpendicular) to the b axis, i.e., σ (π) polarization.

The inset of Fig. 1(a) illustrates the projection of the superlattice onto the scattering plane and shows that the magnetic modulation vector \mathbf{Q}_M is not parallel to that of the superlattice structure \mathbf{Q}_L . In comparison with measurements of other manganites,^{12,14,15} the energy scans plotted in Fig. 1(a) indicate that magnetic scattering prevails at energy 640.5 eV at which the scattering from the superlattice structure with $\mathbf{q} = (0 \ 0 \ 2)$ is strongly suppressed, because $2\theta = 75.9^\circ$. Figure 1(b) maps the two-dimensional distribution in the $q_a q_c$ plane taken with 640.5-eV x-rays at 80 K. We found two modulation vectors $(-0.0021 \ 0 \ 1.610)$ and $(-0.0020 \ 0 \ 2.087)$, denoted as $\mathbf{Q}_{1.5}$ and \mathbf{Q}_2 , respectively, corresponding to $(0 \ 0 \ \frac{3}{2})_M$ and $(0 \ 0 \ 2)_M$ of a superlattice grown on a non-miscut substrate; subscript M denotes that \mathbf{Q}_M is expressed in units of $(\frac{2\pi}{a} \ \frac{2\pi}{a} \ \frac{2\pi}{\Lambda_0})$ with Λ_0 being the periodicity of a perfect superlattice, i.e., $\Lambda_0 = 8a$. The energy scans with \mathbf{Q}_M resemble closely those of magnetic scattering of other manganites;

^{a)}Electronic mail: djhuang@nsrc.org.tw.

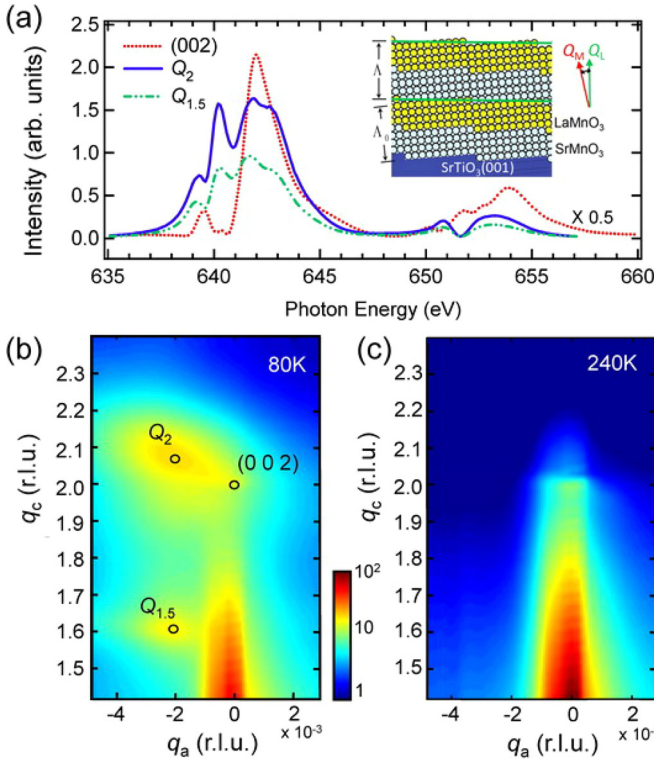


FIG. 1. (Color online) (a) Energy scan of resonant soft-x-ray scattering about the Mn $L_{2,3}$ -edge with q fixed at Q_L , $Q_{1.5}$, and Q_2 . Inset: illustration of the projection of the superlattice onto the scattering plane. (b) and (c) Intensity map of magnetic scattering in the $q_a q_c$ plane measured with 640.5-eV x-rays at 80 and 240 K. Q_L , $Q_{1.5}$, and Q_2 are, respectively, $(0\ 0\ 2)$, $(-0.0021\ 0\ 1.610)$, and $(-0.0020\ 0\ 2.087)$ in units of $(\frac{2\pi}{a}\ \frac{2\pi}{a}\ \frac{2\pi}{\Lambda})$.

these modulation vectors are hence of magnetic origin. In addition, as shown in Fig. 1(c), the scattering intensity with Q_M vanishes above the Néel temperature (T_N) of SrMnO₃, lending further support for its magnetic origin.

Temperature-dependent measurements of magnetic scattering plotted in Fig. 2(a) show magnetic transitions of the LaMnO₃/SrMnO₃ superlattice. As the temperature decreases, the scattering intensities of the half-order Q_M ($Q_{1.5}$ and $Q_{2.5}$) begin to emerge at $T_{N1} = 220$ K, whereas those of Q_2 and Q_3 appear at a $T_{N2} = 198$ K. The clear disparity between the two transitions provides incontestable evidence for two distinct

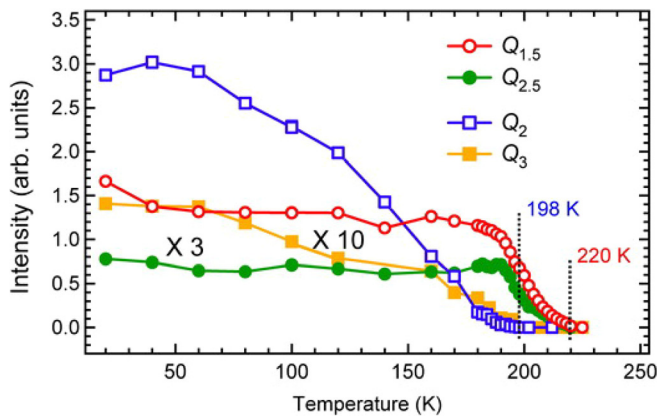


FIG. 2. (Color online) Temperature-dependent measurements of magnetic scattering with varied Q_M . $Q_{1.5}$, Q_2 , $Q_{2.5}$, and Q_3 are, respectively, $(-0.0021\ 0\ 1.610)$, $(-0.0020\ 0\ 2.087)$, $(-0.0024\ 0\ 2.604)$, and $(-0.0023\ 0\ 3.104)$ in units of $(\frac{2\pi}{a}\ \frac{2\pi}{a}\ \frac{2\pi}{\Lambda})$.

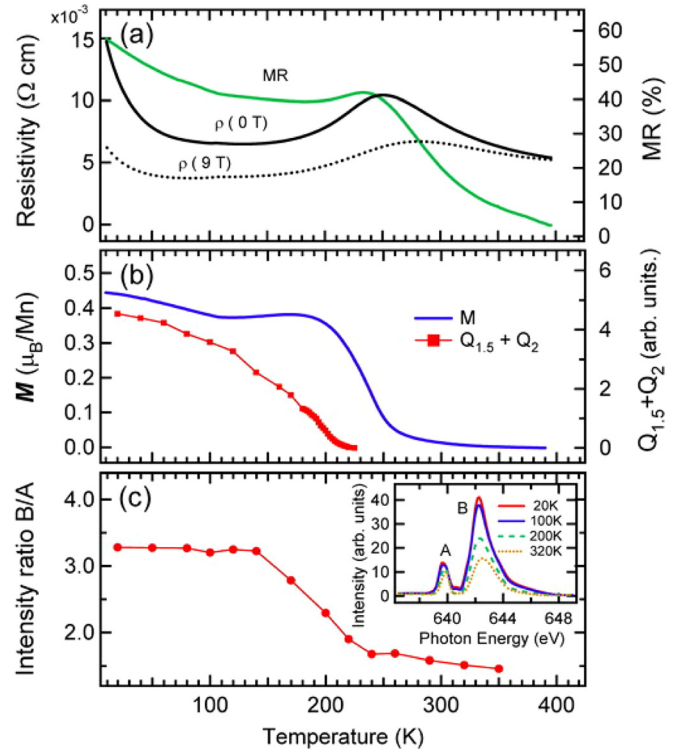


FIG. 3. (Color online) (a) In-plane resistivity ρ recorded with magnetic fields 0 and 9 T and magnetoresistance (MR) vs. temperature. (b) Temperature dependence of x-ray magnetic scattering with $Q_{1.5} + Q_2$ and magnetization obtained with a SQUID magnetometer using in-plane magnetic field 0.05 T. (c) Temperature dependence of intensity ratio B/A measured with π polarization and $q = (002)$, which reflects the JT distortion. Inset: plots of energy scan recorded at various temperatures.

magnetic orders in the superlattice. In addition, the in-plane resistivity of the superlattice exhibits a crossing from insulating to metallic behavior^{16,17} at $T_{MI} = 250$ K, and the magnetization M measured with a superconducting quantum interference device (SQUID) under a magnetic field 0.05 T appears at T_{MI} , as plotted in Figs. 3(a) and 3(b). These observations indicate that, upon cooling across 250 K, the magnetization of the superlattice without interlayer coupling develops before the formation of three-dimensional AFM ordering.

To understand the observed magnetic transitions of the superlattice, we propose the following scenario. The onset temperature of the superlattice magnetism is 250 K. Between 250 and 220 K, there is no interlayer magnetic coupling and the most likely is the existence of interfacial magnetization for lack of magnetic peaks in the scattering measurement. As the temperature is cooled across 220 K, the existence of half-order Q_M implies an antiferromagnetic alignment or a fluctuation in the magnitude of the net magnetization. Such a magnetization results probably from the magnetic coupling in SrMnO₃, because bulk LaMnO₃ and SrMnO₃ are A- and G-type AFM insulators with the Néel temperatures 140 and 233 K, respectively. With the further decrease of temperature across 198 K, the magnetization of LaMnO₃ produces the onset of the integer Q_M peaks.^{18,19}

After establishing the magnetic transition, we examined the influence of magnetization on JT and orbital orderings by choosing the periodicity $\Lambda \approx 8a$ to suppress charge scattering as illustrated in Fig. 4(a). Because $(\epsilon_1 \cdot \epsilon_2)^2 = 0.059$ for π polarization, the resonant scattering of $q = (0\ 0\ 2)$

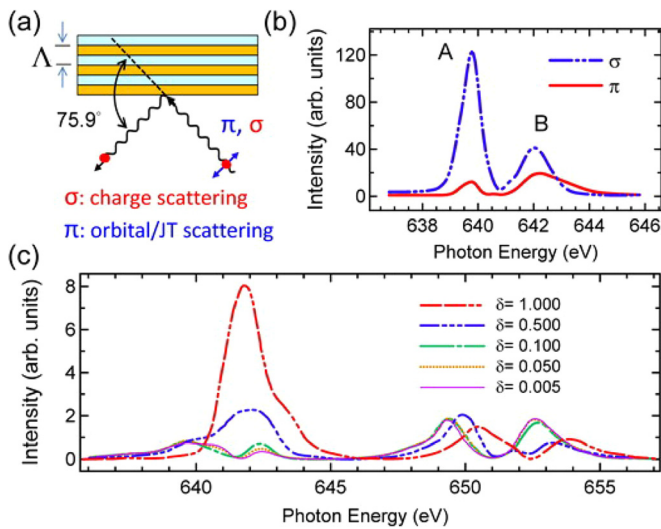


FIG. 4. (Color online) (a) Illustration of scattering with periodicity $\Lambda = 8a$ chosen to suppress charge scattering. The scattering angle of $q = (0\ 0\ 2)$ was 75.9° . (b) Energy scans of resonant x-ray scattering of π and σ polarizations with $q = (0\ 0\ 2)$ measured at 200 K. (c) Calculated spectra of resonant scattering for selected JT distortions denoted by δ (reproduced from Ref. 20).

measured at the Mn L_3 -edge with π polarization is dominated by orbital/JT scattering. The presence of two peaks at 639 and 642 eV in the energy scan plotted in Fig. 4(b), labeled A and B, respectively, fully agrees with atomic multiplet calculations. As shown in Fig. 4(c), Castleton and Altarelli²⁰ concluded that peak A arises from orbital ordering and is insensitive to the JT distortion, whereas peak B is due to transitions into the split $t_{2g\downarrow}$ levels with an intensity that is instead sensitive to the JT distortion. The intensity ratio between peaks A and B, thus, yields an experimental means to assess whether the JT distortion alters across the magnetic transition of the superlattice.

The inset of Fig. 3(c) plots the L_3 -edge resonant soft x-ray scattering of $q = (0\ 0\ 2)$ measured with π polarization at various temperatures. To capture the correlation between JT distortion and spin ordering, we compare the temperature evolution of ratio B/A plotted in Fig. 3(c) with those of magnetic scattering, in-plane resistivity, and magnetization M . Ratio B/A exhibits a strong enhancement at the onset of the magnetization, providing direct evidence of strong correlation between the global JT distortion and spin ordering in the superlattice.

The observation of the enhanced JT distortion with spin ordering reveals its many-body origin, as the spin order is

driven mainly by the electronic correlations. A plausible scenario for the cooperative JT distortion thus emerges: electron-phonon interactions cause local JT distortions, but they rely on both electron-electron and electron-phonon interactions to achieve global alignment. This picture explains why the local JT distortions persist at high temperatures at which both spin and orbital orderings are absent. It also justifies the correlated enhancement of JT distortion across the transition temperatures of spin and orbital orderings.

We thank A. Fujimori and C. Y. Mou for valuable discussions and staffs of NSRRC for technical support. National Science Council of Taiwan in part supported this work. This work was also partially supported by Grant-in-Aid for Scientific Research (B) (22340108) of Japan.

- ¹Y. Tokura and N. Nagaosa, *Science* **288**, 462 (2000).
- ²J. Kanamori, *J. Appl. Phys.* **31**, S14 (1960).
- ³K. Kugel and D. Khomskii, *Sov. Phys. JETP* **37**, 725 (1973).
- ⁴X. Qiu, T. Proffen, J. F. Mitchell, and S. J. L. Billinge, *Phys. Rev. Lett.* **94**, 177203 (2005).
- ⁵A. Sartbaeva, S. A. Wells, M. F. Thorpe, E. S. Božin, and S. J. L. Billinge, *Phys. Rev. Lett.* **99**, 155503 (2007).
- ⁶E. Pavarini and E. Koch, *Phys. Rev. Lett.* **104**, 086402 (2010).
- ⁷A. Sadoc, B. Mercey, C. Simon, D. Grebille, W. Prellier, and M.-B. Lepetit, *Phys. Rev. Lett.* **104**, 046804 (2010).
- ⁸J. Rodríguez-Carvajal, M. Hennion, F. Moussa, A. H. Moudden, L. Pinsard, and A. Revcolevschi, *Phys. Rev. B* **57**, R3189 (1998).
- ⁹Y. Murakami, J. P. Hill, D. Gibbs, M. Blume, I. Koyama, M. Tanaka, H. Kawata, T. Arima, Y. Tokura, K. Hirota *et al.*, *Phys. Rev. Lett.* **81**, 582 (1998).
- ¹⁰W.-G. Yin, D. Volja, and W. Ku, *Phys. Rev. Lett.* **96**, 116405 (2006).
- ¹¹J. P. Hannon, G. T. Trammell, M. Blume, and D. Gibbs, *Phys. Rev. Lett.* **61**, 1245 (1988).
- ¹²D.-J. Huang, J. Okamoto, S.-W. Huang, and C.-Y. Mou, *J. Phys. Soc. Jpn.* **79**, 011009 (2010).
- ¹³J. Okamoto, D. J. Huang, C.-Y. Mou, K. S. Chao, H.-J. Lin, S. Park, S.-W. Cheong, and C. T. Chen, *Phys. Rev. Lett.* **98**, 157202 (2007).
- ¹⁴N. Stojić, N. Binggeli, and M. Altarelli, *Phys. Rev. B* **72**, 104108 (2005).
- ¹⁵U. Staub, V. Scagnoli, A. M. Mulders, K. Katsumata, Z. Honda, H. Grimmer, M. Horisberger, and J. M. Tonnerre, *Phys. Rev. B* **71**, 214421 (2005).
- ¹⁶S. Smadici, P. Abbamonte, A. Bhattacharya, X. Zhai, B. Jiang, A. Rusydi, J. N. Eckstein, S. D. Bader, and J.-M. Zuo, *Phys. Rev. Lett.* **99**, 196404 (2007).
- ¹⁷A. Bhattacharya, S. J. May, S. G. E. te Velthuis, M. Warusawithana, X. Zhai, B. Jiang, J.-M. Zuo, M. R. Fitzsimmons, S. D. Bader, and J. N. Eckstein, *Phys. Rev. Lett.* **100**, 257203 (2008).
- ¹⁸K. Hirota, N. Kaneko, A. Nishizawa, and Y. Endoh, *J. Phys. Soc. Jpn.* **65**, 3736 (1996).
- ¹⁹O. Chmaissem, B. Dabrowski, S. Kolesnik, J. Mais, D. E. Brown, R. Kruk, P. Prior, B. Pyles, and J. D. Jorgensen, *Phys. Rev. B* **64**, 134412 (2001).
- ²⁰C. W. M. Castleton and M. Altarelli, *Phys. Rev. B* **62**, 1033 (2000).